fects in SIMOX devices[6] as well as to hot electron degradation of SIMOX transistor back channel characteristics.

Acknowledgments

The contributions of G. A. Brown and A. G. Revesz were supported by Naval Research Laboratory. Reference 14 was provided by R. J. Lambert.

Manuscript submitted Dec. 2, 1993; revised manuscript received May 2, 1994.

Texas Instruments assisted in meeting the publication costs of this article.

REFERENCES

1. J.-P. Colinge, *Silicon-on-Insulator Technology,* Kluwer Academic Pub., Norwell, MA (1991).
2. A. G. Revesz, G. A. Brown, and H. L. Hughes, in *Amorphous Thin Insulating Films,* J. Kanicky, W. L. Warren, R. A. B. Devine, and M. Matsumura, Editors, MRS Symp. Proc., Vol. 284 (1992).
3. P. K. Hurley, S. Hall, and W. Eccleston, *IEEE Electron Device Lett.,* **EDL-13,** 238 (1992).
4. R. K. Lawrence, H. L. Hughes, and A. G. Revesz, in *Proceedings of 1992 IEEE/SOI Conference,* p. 106, IEEE (1992).
5. A. G. Revesz, G. A. Brown, and H. L. Hughes, *This Journal,* **140,** 3222 (1993).
6. R. E. Stahlbush, G. J. Campisi, J. B. McKitterick, W. P. Maszara, P. Roitman, and G. A. Brown, *IEEE Trans. Nucl. Sci.,* **NS-39,** 2086 (1992).
7. D. J. DiMaria, *J. Appl. Phys.,* **47,** 4073 (1976).
8. T. H. Ning and H. Yu, *ibid.,* **45,** 5373 (1974).
9. T. H. Ning, *ibid.,* **49,** 4077 (1978).
10. V. K. Adamchuk and V. V. Afanas'ev, *Progr. Surf. Sci.,* **41,** 111 (1992).
11. S. I. Fedosenko, V. K. Adamchuk, and V. V. Afanas'ev, *Microelectronics Eng.,* **22,** 367 (1993).
12. D. J. DiMaria, D. W. Dong, C. Falcony, T. N. Theis, J. R. Kirtley, J. C. Tsang, D. R. Young, and F. L. Pesavento, *J. Appl. Phys.,* **54,** 5801 (1983).
13. F. J. Feigl, D. R. Young, D. J. DiMaria, S. Lai, and J. Calise, *ibid.,* **52,** 5665 (1981).
14. R. J. Lambert, T. N. Bhar, and H. L. Hughes, in *Proceedings of 1993 IEEE/SOI Conference,* p. 70, IEEE (1993).
15. D. Fathy, O. L. Krivanek, R. W. Carpenter, and S. R. Wilson, *Inst. Phys. Conf. Ser.,* No. 67: Sect. 10, p. 479 (1983).

Thermal Stability of $Cu/CoSi_2$ Contacted p^+n Shallow Junction with and without TiW Diffusion Barrier

Jung-Chao Chiou and Mao-Chieh Chen*

Department of Electronics Engineering and the Institute of Electronics, National Chiao-Tung University, Hsinchu, Taiwan

ABSTRACT

The thermal stability of $Cu/CoSi_2$ contacted p^+n shallow junction diodes with and without TiW diffusion barrier was investigated with respect to metallurgical reaction and electrical characteristics. Without the diffusion barrier, the Cu (2000 Å)/$CoSi_2$ (700 Å)/p^+n diodes (with a junction depth of 0.2 μm measured from the silicide surface) were able to sustain a 30 s rapid thermal annealing (RTA) in N_2 ambient up to 450°C without losing the integrity of the devices characteristics. The Cu_3Si phase was observed at the $CoSi_2$/Si interface after 500°C annealing; the phase penetrated through the $CoSi_2$ layer causing a catastrophic change in layer structure after 700°C annealing. With the addition of a 1200 Å thickness of TiW diffusion barrier between Cu and $CoSi_2$, the junction diodes were able to sustain the RTA treatment up to 775°C without degrading the basic electrical characteristics, and no metallurgical reaction could be observed even after an 800°C annealing.

Copper has been regarded as a potential metallization material in deep submicron integrated circuits because of its low resistivity (1.67 μΩ-cm for bulk) and superior high electromigration resistance.[1,2] However, copper forms Cu-Si compounds at very low temperatures (200°C).[3-7] The high diffusivity of Cu will also introduce deep level traps in Si that deteriorate the device performance.[8] To make the Cu as an interconnect metal for Si devices, the thermal reaction of Cu with the underlayer materials and devices must be carefully evaluated.

Since silicides have been widely used as contact materials in ultralarge scale integrated (ULSI) circuits, many studies have been made on Cu/silicide systems and their diffusion barriers properties.[9-15] It has been reported that Cu reveals different reaction behavior with different silicides.[16] Copper was found to diffuse across the silicide layer and form the Cu-Si compound below the silicide layers in the $Cu/CrSi_2$/Si and $Cu/CoSi_2$/Si systems; on the other hand, Si is the dominant diffusing species and diffuses out to react with Cu to form Cu_3Si in the $Cu/TiSi_2$/Si structure. Apart from the interdiffusion through the silicide layer, Cu was also found to react with the silicide layer in the $Cu/TiSi_2$/Si system.[16] Because the reaction in the Cu/silicide/Si structure is so complicated and always occurs at relatively low temperature, a more detailed understanding on the reaction mechanism is desirable, and an effective diffusion barrier layer is required for the application of the Cu/silicide structure.

The diffusion barriers employed directly in between the Cu and Si substrate have been widely investigated these days, and most of the results are summarized in Ref. 17. Among the various diffusion barriers, $Ti_{0.27}W_{0.73}$ has been

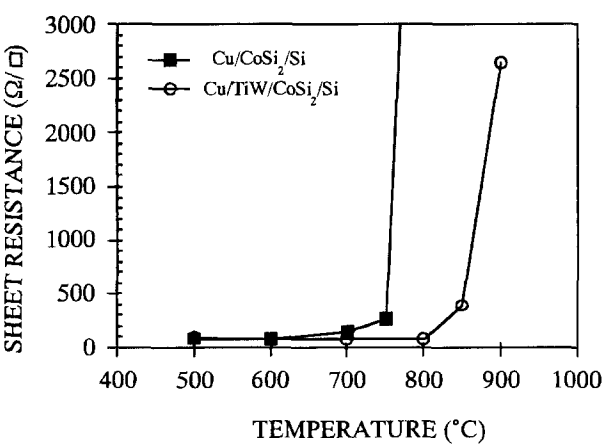

Fig. 1. Sheet resistance vs. annealing temperature for the Cu (2000 Å)/$CoSi_2$ (700 Å)/Si and Cu (2000 Å)/TiW (1200 Å)/$CoSi_2$ (700 Å)/Si samples.

* Electrochemical Society Active Member.

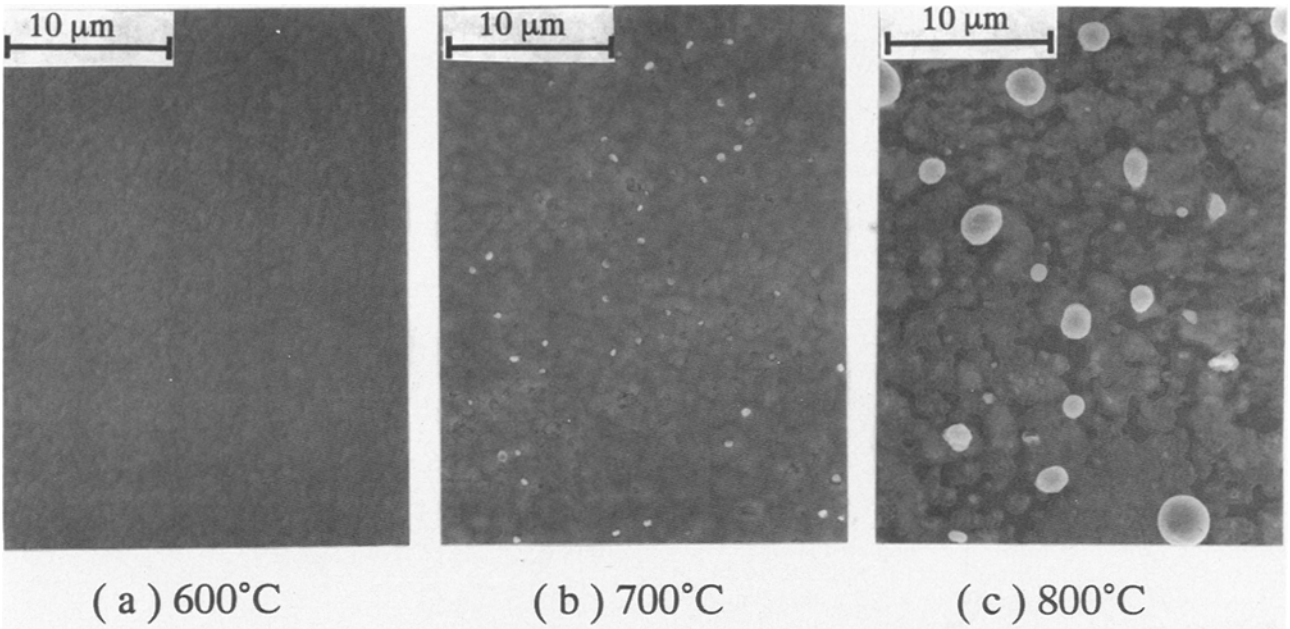

Fig. 2. SEM micrographs showing surface morphology for the RTA (in N_2 for 30 s) annealed Cu (2000 Å)/$CoSi_2$ (700 Å)/Si structure at a temperature of (a) 600, (b) 700, and (c) 800°C.

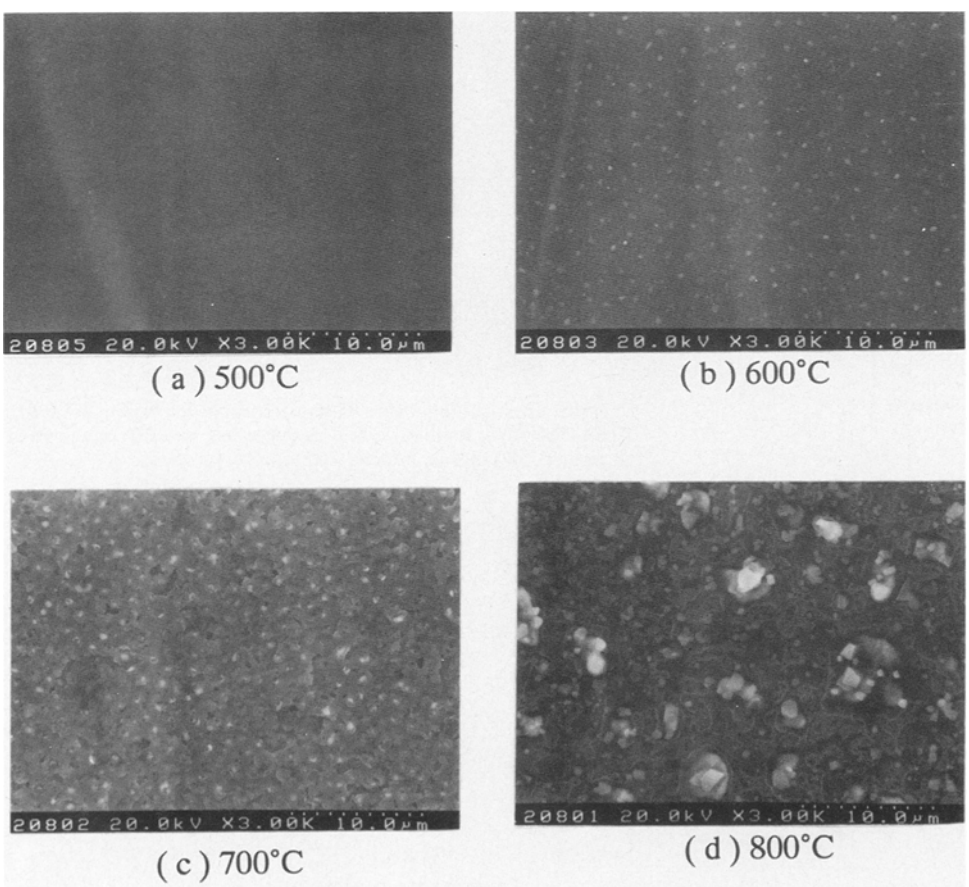

Fig. 3. SEM micrographs of $CoSi_2$ after removal of the Cu film from the RTA annealed Cu (2000 Å)/$CoSi_2$ (700 Å)/Si samples. The annealing temperatures are (a) 500, (b) 600, (c) 700, and (d) 800°C.

regarded as a very effective one for the Cu/TiW/Si system.[17] In addition, it has been reported that TiW (Ti:W = 10:90 w/o) is also an effective diffusion barrier material for the Al/TiW/$CoSi_2$/Si system.[18] Since $CoSi_2$ has been regarded as one of the promising silicides in future ULSI application,[19,20] we investigate, in this work, the thermal stability of the Cu/$CoSi_2$/p^+n as well as the Cu/TiW/$CoSi_2$/p^+n junction diodes in both metallurgical and electrical respects.

Experimental Procedure

Samples were fabricated on n-type (100)-oriented silicon wafers with 1 to 10 Ω-cm nominal resistivity. After standard cleaning, 5000 Å SiO_2 was thermally grown in a pyrogenic steam atmosphere at 1050°C for 90 min. Square active regions with area of 2.5×10^{-3} cm^2 were defined by the conventional photolithographic method. A cobalt film of 200 Å thickness was deposited in an E-beam evaporation system. Without breaking the vacuum, a 50 Å thickness of

α-Si was deposited on top of the Co film to serve as a passivation film for preventing the cobalt from reacting with oxygen during the cobalt silicide formation. The samples were then annealed at 550°C for 30 min in a normal nitrogen-flowing furnace to form $CoSi_2$ of about 700 Å thickness in the active areas. The unreacted Co was selectively etched in a 1:1:6 mixture of $HCl:H_2O_2:H_2O$. The p^+n junctions were formed by BF_2^+ implantation at 70 keV to a dose of 5×10^{15} cm^{-2} through $CoSi_2$ followed by annealing at a temperature of 700°C for 90 min in N_2 ambient. The junction made by this process was estimated to be 0.2 μm measured from the silicide surface.[21] A 1200 Å thick TiW diffusion barrier layer was deposited on a group of the samples. The deposition was carried out by sputtering using the TiW [Ti 10 weight percent (w/o)] target in Ar ambient at a pressure of 5×10^{-3} Torr and with a deposition rate of 1.7 Å/s. All of the samples, with and without the TiW layers, were exposed to air before Cu deposition. A Cu film of 2000 Å thickness was then deposited on all samples (with and without the TiW layers) by sputtering the Cu (99.99%) target in Ar ambient at a pressure of 5×10^{-3} Torr and with a deposition rate of 0.1 Å/s. The completed samples were then treated with rapid thermal annealing (RTA) for 30 s at temperatures ranging from 300 to 900°C with a temperature ramping of 100°C/s in N_2 ambient. Finally, the backside of the wafers was metallized by Al deposition for electrical measurement. Unpatterned samples of $Cu/CoSi_2/Si$ and $Cu/TiW/CoSi_2/Si$ structures were also prepared following the same processing sequence and annealing treatment for material analysis. Sheet resistance was measured by four-point probe on the unpatterned samples. The surface morphologies were inspected by scanning electron microscope (SEM). Scanning Auger microscope (SAM) was employed for depth profile structure analysis. The material phases were identified by glancing angle (1°) x-ray diffraction. The transmission electron microscope (TEM) was used for revealing the interaction in the layered structures. The electrical characteristics of the diodes were measured by a semiconductor parameter analyzer HP4145B.

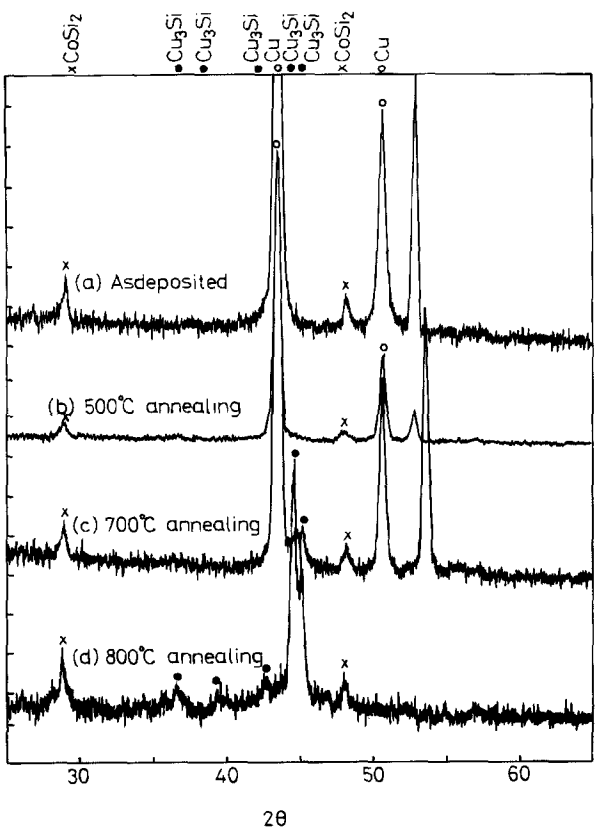

Fig. 4. The glancing angle (1°) XRD pattern for the Cu (2000 Å)/$CoSi_2$ (700 Å)/Si sample: (a) as-deposited, and RTA annealed at (b) 500, (c) 700, and (d) 800°C in N_2 for 30 s.

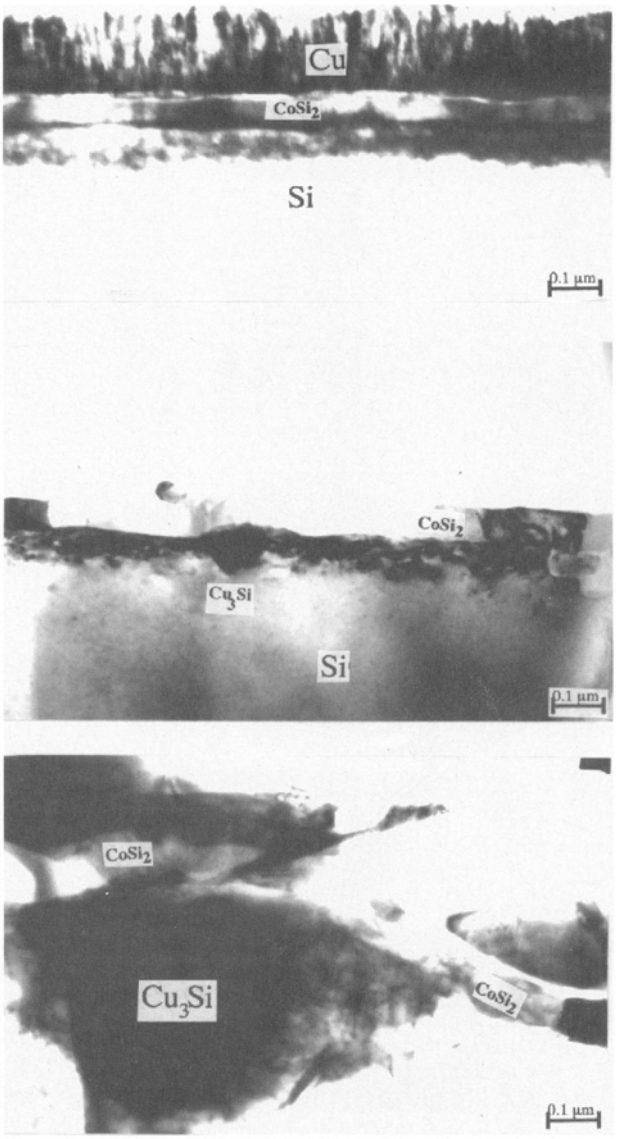

Fig. 5. Cross-sectional view TEM micrographs for the Cu (2000 Å)/$CoSi_2$ (700 Å)/Si sample: (a, top) as-deposited, and RTA annealed at (b, center) 500 and (c, bottom) 700°C in N_2 for 30 s.

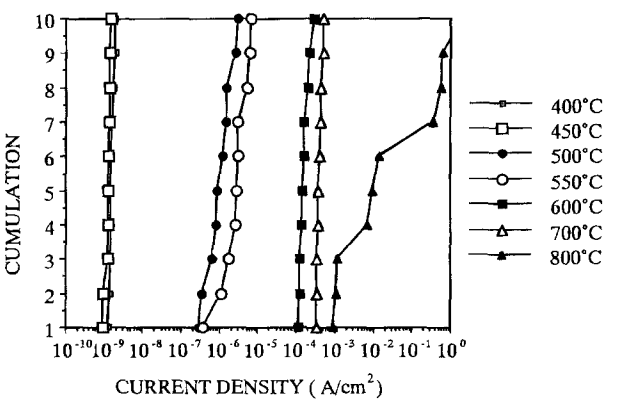

Fig. 6. Statistic cumulation of the reverse leakage current densities for the RTA annealed Cu (2000 Å)/$CoSi_2$ (700 Å)/Si p^+n junction diodes.

Results and Discussion

$Cu/CoSi_2/Si$.—The sheet resistance R_s of the $Cu/CoSi_2/Si$ and the $Cu/TiW/CoSi_2/Si$ structures after RTA annealing in N_2 for 30 s at various temperatures is illustrated in Fig. 1.

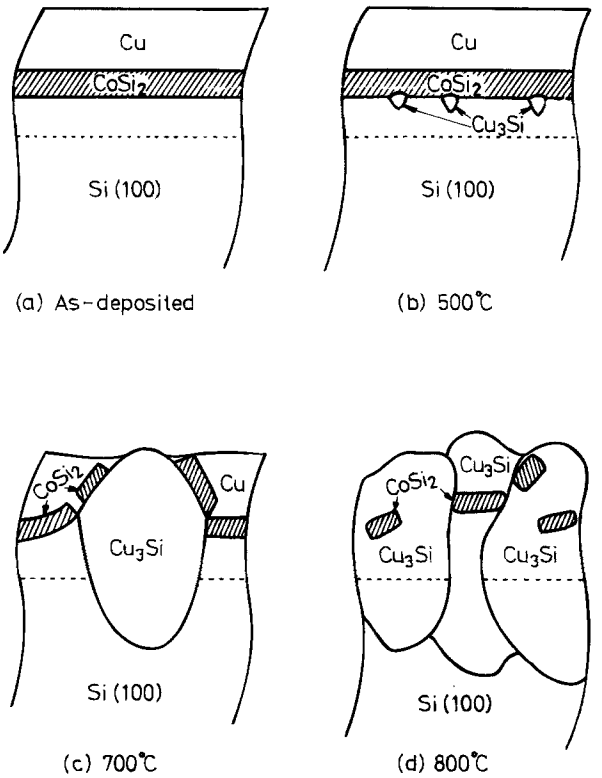

Fig. 7. Schematic diagrams showing the $Cu/CoSi_2/Si$ structure: (a) as-deposited and after RTA annealing at (b) 500, (c) 700, and (d) 800°C.

The R_s for the Cu (2000 Å)/$CoSi_2$ (700 Å)/Si structure does not change up to 600°C RTA annealing. Since the Cu film is thicker and has a much lower resistivity than $CoSi_2$, the stable value of R_s indicates that the Cu film in the Cu/$CoSi_2$/Si structure remains intact up to 600°C. A sharp increase of R_s was observed after annealing at 700°C indicating that a structural change had occurred after this annealing. The SEM micrographs showing the surface morphology of the annealed $Cu/CoSi_2/Si$ structures are illustrated in Fig. 2. On the 700°C annealed sample, some precipitate (white dots) and circular-shaped local defects were observed on the Cu surface. After 800°C annealing, a complete color change of surface from reddish yellow (Cu) to silver gray could be seen by the naked eye and the sample surface was composed of discontinuous film structure in which large precipitates appeared. The SEM micrographs for the $CoSi_2$ surface after removal of the Cu layer by the $HCl + H_2O_2 + H_2O$ (1:1:6) solution are shown in Fig. 3. Precipitate was found on the 500°C annealed sample, and this precipitate became larger after 600°C annealing. After 700°C annealing, the precipitate grew even larger and a collapsed structure can be observed; the collapsed structure is consistent with the defect shown in Fig. 2b. The 800°C annealed sample shows a discontinuous film structure similar to that shown in Fig. 2c; furthermore, it can be seen that the precipitate is seemingly grown from the underlying silicon substrate.

The glancing angle (1°) x-ray diffraction result is shown in Fig. 4. It reveals that Cu_3Si phase appeared in the 700°C annealed sample. After 800°C annealing, all of the Cu reacted completely with Si to form Cu_3Si, while the $CoSi_2$ phase notably remained. From the above observation, it can be inferred that the precipitate on the surface must be Cu_3Si, and that this Cu-Si compound formation must be responsible for the increase of sheet resistance.

The AES depth profile (not shown) indicates that no apparent structure intermixing occurred in the $Cu/CoSi_2/Si$ structure up to 700°C annealing. However, the structure was completely destroyed after 800°C annealing.

The cross-sectional TEM micrographs, as shown in Fig. 5, provide a direct observation on the inner structure. Figure 5a shows the cross-sectional view of an as-deposited sample. After 500°C annealing, triangular-shaped precipitates can be observed at the interface between $CoSi_2$ and Si, as shown in Fig. 5b. The precipitation was usually found in the Cu/silicide system and was identified as the Cu_3Si phase which is usually surrounded by amorphous SiO_2.[22,23] The size of this Cu_3Si precipitate is less than 1000 Å as shown in Fig. 5b. The Cu_3Si phase was not detected in the XRD spectrum presumably because its volume fraction is below the XRD detection limit. After 700°C annealing, a precipitate with size of several thousand angstroms can be found under the $CoSi_2$ layer and some of the precipitate entered the Cu film by breaking the $CoSi_2$ layer. The precipitate that broke through $CoSi_2$ layer and even reached the top surface of the Cu layer constitutes the white dots observed in Fig. 2b.

The reverse leakage current density measured at −5 V for ten randomly chosen samples is illustrated in Fig. 6. It is seen that the junction starts to degrade after 500°C annealing. After that, the leakage current increases with the increased annealing temperature.

A clear picture of the reactions occurring in the $Cu/CoSi_2/Si$ structure can be constructed based on the above

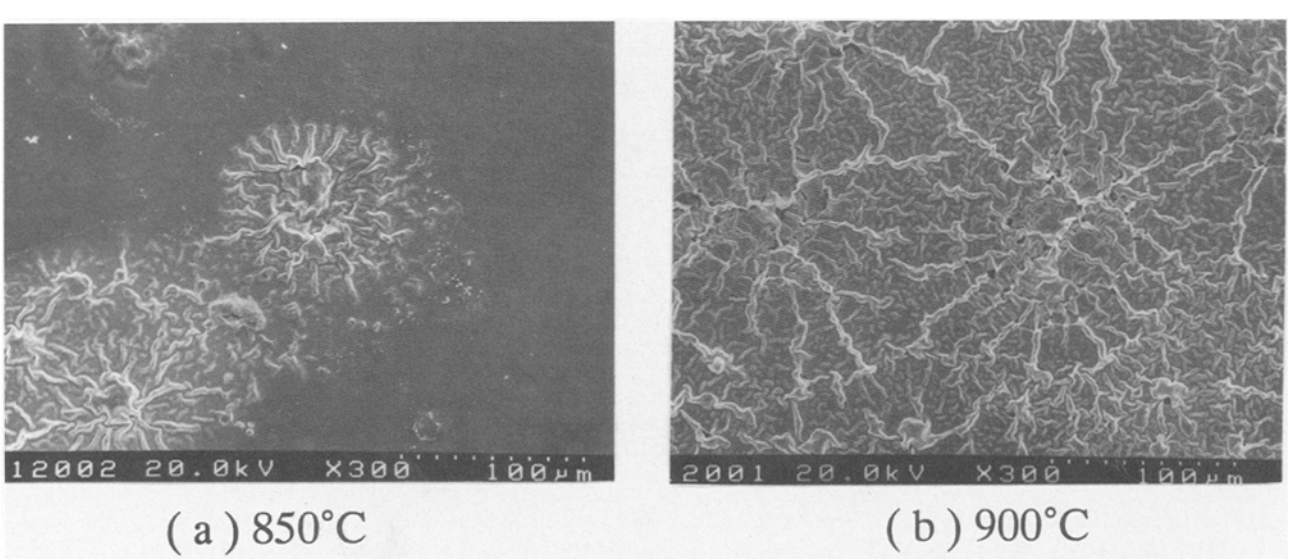

Fig. 8. SEM micrographs showing surface morphology for the RTA (in N_2 for 30 s) annealed Cu (2000 Å)/TiW (1200 Å)/$CoSi_2$ (700 Å)/Si structure at a temperature of (a) 850 and (b) 900°C.

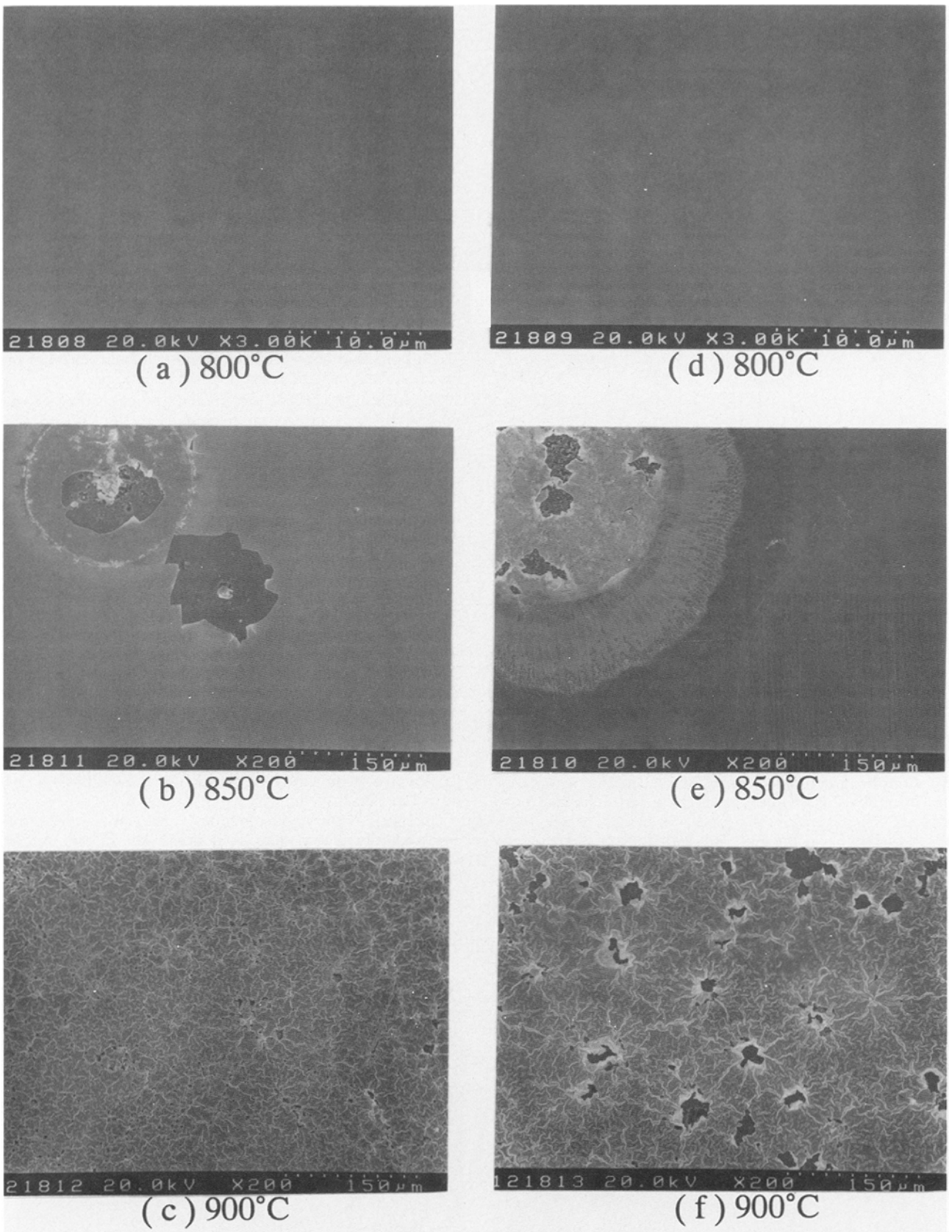

Fig. 9. SEM micrographs showing surface morphology for the RTA (in N_2 for 30 s) annealed Cu (2000 Å)/TiW (1200 Å)/$CoSi_2$ (700 Å)/Si sample after removal of Cu and TiW layers. The Cu was removed from the samples annealed at (a) 800; (b) 850; and (c) 900°C; both Cu and TiW were removed from the samples annealed at (d) 800, (e) 850, and (f) 900°C.

experimental results as shown in Fig. 7. The junction remains intact up to 450°C annealing. After 500°C annealing, a small amount of Cu penetrates through the $CoSi_2$ layer to form the Cu_3Si phase at the interface of $CoSi_2$/Si. Because the $CoSi_2$ has a column grain structure, the penetration may occur by the grain boundary diffusion. At this stage, the volume fraction of the Cu_3Si phase is too small to be detected by the glancing angle x-ray diffraction. Thus, the sample's sheet resistance and the $CoSi_2$ layer are not significantly affected by this small precipitate. However, a dra-

matic change happens to the structure after 700°C annealing. The Cu_3Si phase, at this temperature, has grown big enough to pierce through the $CoSi_2$ layer and even reach the top surface of the Cu film. The amount of Cu_3Si phase after 700°C annealing can be easily detected by the XRD. After 800°C annealing, the Cu_3Si breaks the $CoSi_2$ layer and appears across the layer structure. The $CoSi_2$ layer, though pierced by the Cu_3Si, seemly keeps phase stable. The schematic diagram given in Fig. 7 illustrates this mechanism.

Cu/TiW (1200 Å)/$CoSi_2$/Si.—The sheet resistance for Cu (2000 Å)/TiW (1200 Å)/$CoSi_2$ (700 Å)/Si structure, as shown in Fig. 1, indicates that it remains stable up to 800°C annealing. After 850°C annealing, some local spot areas of silver-gray color can be observed by the naked eye accompanied by an R_s increase. After 900°C annealing, the R_s made a dramatic increase, and the sample surface completely changed from reddish yellow to silver-gray color. The SEM micrographs in Fig. 8 show that the silver-gray area contains local defects featuring a radial pattern of cracks. This crack structure spreads and covers the entire surface after 900°C annealing (Fig. 8b). Similar radial looking grain structures centered at "reaction spot" was observed in the Cu/TiW/Si system after a 800°C 30 s RTA annealing.[17] Figure 9 shows the SEM surface morphologies for the RTA-annealed Cu/TiW/$CoSi_2$/Si samples after removal of Cu and TiW layers by the HCl + H_2O_2 + H_2O (1:1:6) and NH_4OH + H_2O_2 + H_2O (1:1:1) solutions, respectively. Both surfaces of TiW and $CoSi_2$ remain intact for the 800°C annealed sample. The 850°C annealed sample (Fig. 9b and e) reveals local reactive spots deeply penetrated into the TiW and $CoSi_2$ layers. The radial grain structure on the 900°C annealed sample (Fig. 9c and f) apparently has not been removed by the removal of the Cu and TiW layers, as is obvious by comparing Fig. 8b with Fig. 9c and 9f.

The XRD pattern, as shown in Fig. 10, exhibits new phases surely formed after 850°C annealing. The new phases on the 850°C annealed sample were identified as Cu_3Si and WSi_2. After 900°C annealing, all of the Cu and TiW phases vanish, and the existent major compounds are Cu_3Si, WSi_2, and $(Ti_{0.6}W_{0.4})Si_2$. The WSi_2 and $(Ti_{0.6}W_{0.4})Si_2$ are the phases that usually appeared at the TiW/Si system.[24-26] However, W_5Si_3 and Ti_5Si_3 or Ti_5Si_4 were found in the $Cu/Ti_{0.27}W_{0.73}/Si$ system.[17] The XRD results also indicate that the $CoSi_2$ phase remains stable up to 900°C annealing, though catastrophic reaction has occurred at such a high temperature. The lattice constant of the as-deposited bcc structure TiW film deduced from the XRD pattern is 3.175 Å, and this constant did not change after 800°C annealing. However, the lattice constant shifted to 3.189 Å after 850°C annealing. Since the atomic radii of W (bcc) and Ti (hcp) are

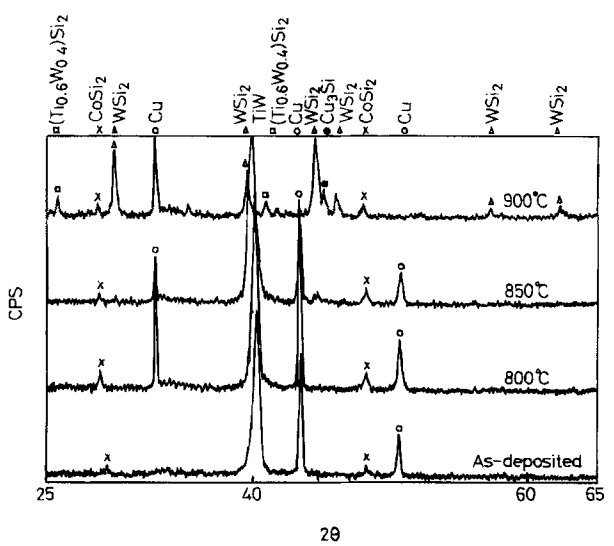

Fig. 10. The XRD spectra for the Cu (2000 Å)/TiW (1200 Å)/$CoSi_2$ (700 Å)/Si sample: as-deposited and RTA annealed at 800, 850, and 900°C in N_2 for 30 s.

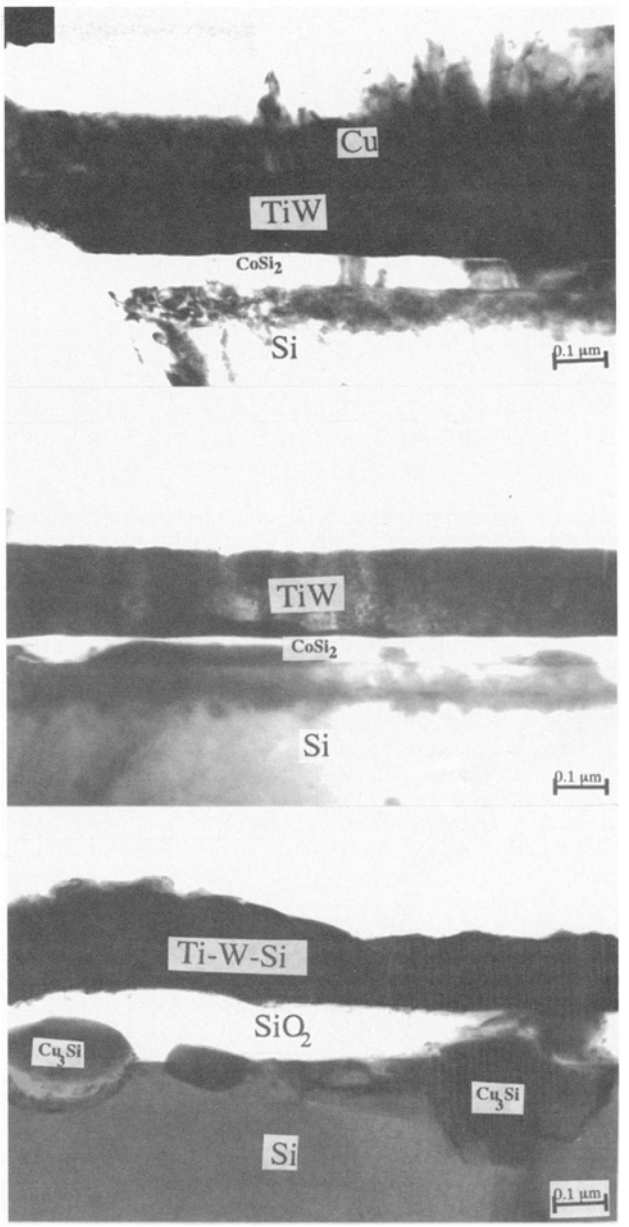

Fig. 11. Cross-sectional view of TEM micrographs for the RTA (in N_2 for 30 s) annealed Cu (2000 Å)/TiW (1200 Å)/$CoSi_2$ (700 Å)/Si sample at a temperature of (a, top) 800, (b, center) 850, and (c, bottom) 900°C.

1.37 and 1.475 Å, respectively, the lattice constant of TiW (bcc) will be different from that of W because of the Ti addition; that is, the Ti addition will enlarge the lattice parameter of the TiW (bcc) structure. The lattice constant shift was clearly observed by comparing the pure W (a = 3.165 Å) with $Ti_{0.27}W_{0.73}$ (a = 3.208 Å) films.[17] Thus, it is clear that films in this study are very Ti deficient; that is, although the TiW film was sputter deposited from a $Ti_{0.3}W_{0.7}$ target, the lighter Ti atom had much loss during the sputter deposition process. On the other hand, the W concentration in the TiW decreases due to WSi_2 phase formation during the 850°C annealing process. Hence, the lattice constant shifted to 3.189 Å. Furthermore, broadening of the XRD signal for TiW, after 850°C annealing, indicates that the W-Si reaction was not very uniform.

The cross-sectional TEM micrographs, as illustrated in Fig. 11, shows that the Cu/TiW/$CoSi_2$/Si structure remains intact after 800°C annealing. For the 850°C annealed sample, Fig. 11b shows that a thin layer is seemingly existent between the TiW and $CoSi_2$ layers. It should be noted that this micrograph shows the area pertaining to the unreacted region (aside from the local reactive spots) as shown in

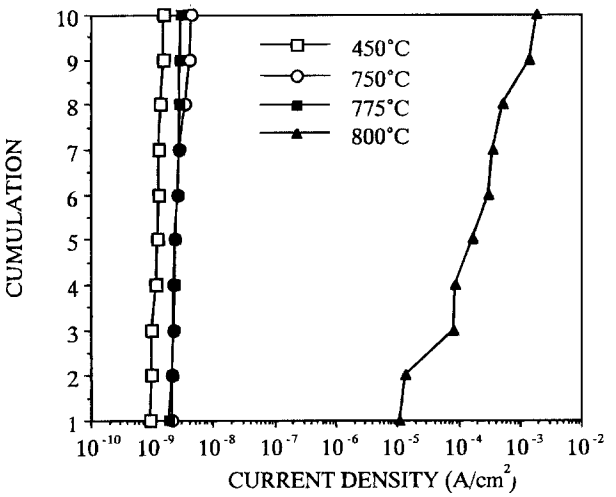

Fig. 12. Statistic cumulation of the reverse leakage current densities for the RTA annealed Cu (2000 Å)/TiW (1200 Å)/$CoSi_2$ (700 Å)/p^+n junction diodes.

Fig. 8a and Fig. 9b and 9e. It is not easy to identify this thin layer and determine how did it occur. The detected Cu_3Si and WSi_2 signals are presumably originated from the reactive region. After 900°C annealing, Cu_3Si precipitation was formed and even penetrated into the Si substrate. It is obvious that most of the Cu transported across TiW and $CoSi_2$ and reacted with the Si substrate. There is a uniform amorphous SiO_2 layer existing on the Cu_3Si precipitate layer. The SiO_2 layer may be induced by the presence of the Cu_3Si phase.[22] The overlaying layer is a Ti-W-Si compound, as shown in Fig. 11c.

The electrical characteristics are usually more sensitive to the reaction which occurred within the structure than the metallurgical properties. The statistical data of the reverse leakage current density for the RTA annealed Cu (200 Å)/TiW (1200 Å)/$CoSi_2$ (700 Å)p^+n junction diodes are illustrated in Fig. 12. The abrupt increase and scattered distribution of leakage current density in the 800°C annealed devices implies that the junctions were markedly destroyed even though no evidence of reaction can be found by the material analysis. It is shown that the electrical property remains basically unchanged up to a 775°C RTA annealing for 30 s. Little metal impurities may diffuse to the junction by the RTA annealing below 775°C.

In the ULSI era, implementation of a junction contact needs to consider the scaling effect. When the contact area is reduced to a size of 10^{-8} cm^2, the metal film thickness would also be changed. The small contact area faces the nonconformal step coverage problem during the metal film deposition by sputtering. The nonconformal silicide and barrier layers within the contact hole with submicrometer size may result in a lower degradation temperature of the contacted junction. In addition, since the extent of the metal-to-barrier reaction depends on the ratio of the volume of metal available for reaction to the area of the contact hole, the realistic implementation that requires 5000 Å thickness of Cu may also cause a slightly lowered degradation temperature. Nonetheless, it can be concluded that the incorporation of TiW diffusion barrier significantly improve the thermal stability of the Cu/$CoSi_2$/Si metallization system.

Conclusion

Copper is used as contact metal in the Cu/$CoSi_2$ (700 Å)/p^+n diodes with a junction depth of 0.2 μm measured from the silicide surface. With a 30 s RTA annealing in N_2 ambient, the diodes' electrical characteristic integrity can be preserved up to a temperature of 450°C. Obvious metallurgical reaction was observed after a 500°C RTA annealing. The Cu_3Si phase first nucleated at the $CoSi_2$/Si interface by the diffusion of Cu through the $CoSi_2$ layer. With a higher temperature annealing of 700°,C, the Cu_3Si grew up to break the $CoSi_2$ layer and caused the structure to collapse. By using a 1200 Å thickness of TiW layer as diffusion barrier, the Cu/TiW/$CoSi_2$ (700 Å)/p^+n diodes were able to sustain the 30 s RTA treatment up to 775°C without degrading the basic electrical characteristic. With a higher temperature annealing of 850°C, metallurgical reaction occurred at local spot areas with the formation of WSi_2, $(Ti_{0.6}W_{0.4})Si_2$, and Cu_3Si phases. Notwithstanding the metallurgical reaction at higher temperature, the incorporation of TiW diffusion barrier in the Cu/$CoSi_2$/Si system makes the structure a potential metallization system in future application.

Acknowledgments

The authors wish to thank the Semiconductor Research Center of National Chiao-Tung University and the National Nano Device Laboratory for providing an excellent processing environment. This work was supported by the National Science Council, ROC, under Contract No. NSC-82-0404-E009-400.

Manuscript submitted Feb. 8, 1994; revised manuscript received April 29, 1994.

The National Chiao-Tung University assisted in meeting the publication costs of this article.

REFERENCES

1. P. L. Pai, C. H. Ting, C. Chiang, C. S. Wei, and D. B. Fraser, *Mater. Res. Soc. Symp. Proc. VLSI-V*, p. 359 (1990).
2. T. E. Seidel, *Mater. Res. Soc. Symp. Proc.*, **260,** 3 (1992).
3. A. Cros, M. O. Aboelfotoh, and K. N. Tu, *J. Appl. Phys.*, **67,** 3328 (1990).
4. S. H. Corn, J. L. Falconer, and A. W. Czanderna, *J. Vac. Sci. Technol.*, **A6,** 1012 (1988).
5. S. Q. Hong, C. M. Comrie, S. W. Russell, and J. W. Mayer, *J. Appl. Phys.*, **70,** 3655 (1992).
6. R. Padiyath, J. Seth, S. V. Babu, and L. J. Matienzo, *ibid.*, **73,** 2326 (1993).
7. L. Stolt, F. M. D'Huerle, and J. M. E. Harper, *Thin Solid Films*, **200,** 147 (1991).
8. S. D. Brotherton, J. R. Ayres, A. Gill, H. W. van Kesteren, and F. J. A. M. Greidanus, *J. Appl. Phys.*, **62,** 1826 (1987).
9. C. A. Chang, *ibid.*, **67,** 6184 (1990).
10. C. A. Chang, *ibid.*, **66,** 2989 (1989).
11. C. A. Chang, *ibid.*, **55,** 754 (1990).
12. C. A. Chang, *ibid.*, **55,** 1543 (1989).
13. C. A. Chang, *ibid.*, **67,** 7348 (1990).
14. C. A. Chang and C. K. Hu, *Appl. Phys. Lett.*, **57,** 617 (1990).
15. C. A. Chang, *J. Vac. Sci. Technol.*, **A8,** 3796 (1990).
16. J. O. Olowolafe, J. Li, and J. W. Mayer, *J. Appl. Phys.*, **68,** 6207 (1990).
17. S. Q. Wang, S. Suthar, C. Hoeflich, and B. J. Burrow, *J. Appl. Phys.*, **73,** 2301 (1993).
18. F. M. Yang and M. C. Chen, *J. Vac. Sci. Technol.*, **B11,** 744 (1993).
19. S. P. Murarka, D. B. Fraser, A. K. Sinha, H. J. Levinstein, E. J. Lloyd, R. Liu, D. S. Williams, and S. J. Hillenius, *IEEE Trans. Electron Devices*, **ED-34,** 2108 (1987).
20. M. A. Farooq, S. P. Murarka, C. C. Chang, and F. A. Baiocchi, *J. Appl. Phys.*, **65,** 3017 (1989).
21. B. S. Chen and M. C. Chen, *ibid.*, **72,** 4619 (1992).
22. K. Holloway, P. M. Fryer, C. Cabral, Jr., J. M. E. Harper, P. J. Bailey, and K. H. Kelleher, *ibid.*, **71,** 5433 (1992).
23. C. B. Liu and L. J. Chen, *ibid.*, **74,** 3611 (1993).
24. B. W. Shen, G. C. Smith, J. M. Anthony, and R. J. Matyi, *J. Vac. Sci. Technol.*, **B4,** 1369 (1986).
25. P. Gas, F. J. Tardy, and F. M. d'Heurle, *J. Appl. Phys.*, **60,** 193 (1986).
26. S. E. Babcock and K. N. Tu, *ibid.*, **53,** 6898 (1982).